Transformation of the multimode terahertz quantum cascade laser beam into a Gaussian, using a hollow dielectric waveguide

Andriy A. Danylov,[1,*] Jerry Waldman,[1] Thomas M. Goyette,[1] Andrew J. Gatesman,[1] Robert H. Giles,[1] Kurt J. Linden,[2] William R. Neal,[2] William E. Nixon,[3] Michael C. Wanke,[4] and John L. Reno[4]

[1]Submillimeter-Wave Technology Laboratory, University of Massachusetts Lowell, Lowell, Massachusetts 01854, USA
[2]Spire Corporation, Bedford, Massachusetts 01730, USA
[3]U.S. Army National Ground Intelligence Center, Charlottesville, Virginia 22911, USA
[4]Sandia National Laboratories, P.O. Box 5800, Albuquerque, New Mexico 87185, USA

*Corresponding author: andriy_danylov@student.uml.edu

Received 5 February 2007; accepted 25 April 2007;
posted 1 June 2007 (Doc. ID 79473); published 9 July 2007

We demonstrate that a short hollow dielectric tube can act as a dielectric waveguide and transform the multimode, highly diverging terahertz quantum cascade laser beam into the lowest order dielectric waveguide hybrid mode, EH_{11}, which then couples efficiently to the free-space Gaussian mode, TEM_{00}. This simple approach should enable terahertz quantum cascade lasers to be employed in applications where a spatially coherent beam is required. © 2007 Optical Society of America

OCIS codes: 140.3070, 140.3300, 140.5960, 230.7370.

1. Introduction

Terahertz quantum cascade lasers (TQCLs) are promising sources for many applications in biomedical imaging [1,2]. They also can be used as local oscillators (LOs) for heterodyne receivers for spectroscopy in atmospheric research [3] and astrophysics [4]. Other important applications include short-range standoff imaging systems for security screening as a means of detecting contraband [5], as well as radar scale modeling [6]. Here, TQCLs could be employed for both the transmitter and LO. Successful TQCL LO results have been reported [4,7] using a superconducting hot-electron bolometer mixer, which requires less than a microwatt of power to be driven.

TQCLs have already produced impressive performance characteristics for LO use, including high cw power levels (up to 138 mW) [8], narrow linewidth (30 kHz) [9], and some tunability. However, the multimode profile [10–12] and high divergence of the output beam from a cavity whose lateral dimensions are comparable to the wavelength present obstacles for LO applications. Consequently, no results of Schottky diode mixer performance using a TQCL as the LO have been reported. At THz frequencies, the Schottky diode is typically mounted in a fundamental waveguide [13] or corner-cube antenna [14,15] and requires a focused, spatially coherent mode of several milliwatts for high receiver sensitivity. In order to achieve good diode performance as a mixer (or even as a direct detector) the amplitude profile and phase of the radiation must match that of the receiver's antenna pattern [16,17]. The goal of this paper is to characterize and shape the TQCL beam profile. We demonstrate that a short hollow Pyrex tube mounted close to the exit facet of the TQCL can act as a dielectric waveguide and transform the multimode, highly diverging TQCL beam into the lowest order dielectric waveguide hybrid mode, EH_{11}, which then couples efficiently to the free-space Gaussian mode, TEM_{00}. Because the initial trial tube has delivered an overall efficiency of approximately 35%, it is anticipated that optimization of this very simple approach will convert at least one-half of the TQCL emitted power into a TEM_{00} mode.

0003-6935/07/225051-05$15.00/0

2. Terahertz Quantum Cascade Laser Fabrication

The TQCL devices were fabricated from sample EA 1249, grown by molecular beam epitaxy at Sandia National Laboratory, with a previously published 2.9 THz epitaxial layer structure [18]. The epitaxial device structure was grown on a semi-insulating GaAs substrate to enable fabrication of devices of the top-metal plasmon confinement waveguide structure. This processing consisted of 100 μm wide ridge formation by chemical etching following Ti/Au ridge-metallization using a liftoff procedure similar to a previously described process [18]. Two Ni/Ge/Au metal contact stripes (each approximately 100 μm wide and separated from the ridge by approximately 100 μm) were then deposited by E-beam evaporation on both sides of the ridge, and the wafer was thinned to approximately 140 μm. Following wafer thinning, the back side of the wafer was also metallized with Ti/Au, but this metallization was only applied to enable soldering of the die to the device package. The back side metal served no electrical function. The wafers were then cleaved into individual laser die, with cavity lengths ranging from 1 mm to 2 mm. For the measurements described in this paper a 1.7 mm cavity with uncoated facets was used.

3. Terahertz Quantum Cascade Laser Characterization

The TQCL is attached to a copper sample holder, which is bolted to an oxygen-free copper plate mounted horizontally in a temperature controlled liquid helium (LHe) dewar [19]. The copper plate is coupled to the LHe cold surface mechanically, through (externally) adjustable jaws. For the measurements reported here the jaws were tightly shut in order to obtain the lowest possible device temperature (approximately 10 K). The TQCL output beam is centered on a 1 inch (25 mm) diameter high-density polyethylene (HDPE) external window, which is approximately 25 mm from the facet of the TQCL. The laser was driven by square wave pulses at the following default settings: bias 4.1 V, frequency 30 Hz, and pulse width 1 ms. The current through the device was approximately 0.3 A. TQCL emission is linearly polarized along the growth direction, which corresponds to the vertical direction in this setup.

The TQCL spectrum was measured using a Fourier transform spectrometer at 0.15 cm^{-1} resolution, in the step-scan mode. The detector was a LHe cooled silicon (Si) bolometer of the composite type. As seen from Fig. 1, the emission is principally from a longitudinal mode positioned at 2.960 THz ($\lambda = 101.4$ μm). Two weaker longitudinal modes can also be seen in Fig. 1.

The laser pulse power was obtained with an absolute power meter [20]. The large detector area allows collection of nearly all the TQCL radiation emerging from the dewar window. The output power was corrected by a factor of 16.7, the duty cycle difference between the power meter calibration (50%) and the TQCL pulsed signal (3%). The laser starts emitting at 3.6 V and stops at 4.5 V, reaching the maximum power of 3.6 mW at 4.4 V.

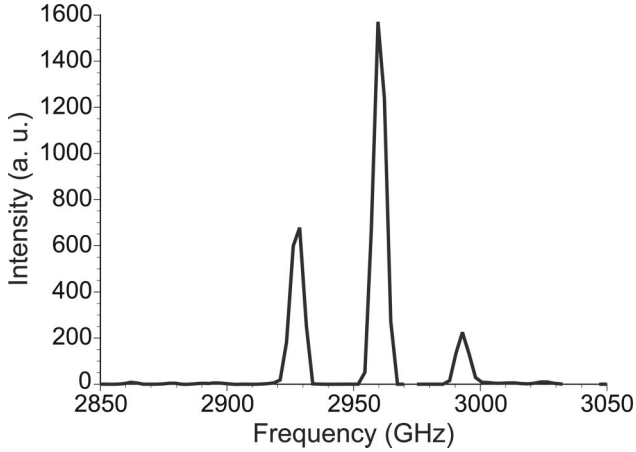

Fig. 1. Emission spectrum of the QCL with a spectrometer resolution of 4.5 GHz.

The beam profile of the TQCL has been measured at several distances from the laser by a linearly translated Si LHe cooled bolometer with steps of 0.3 mm, using a computer-controlled translation stage. The

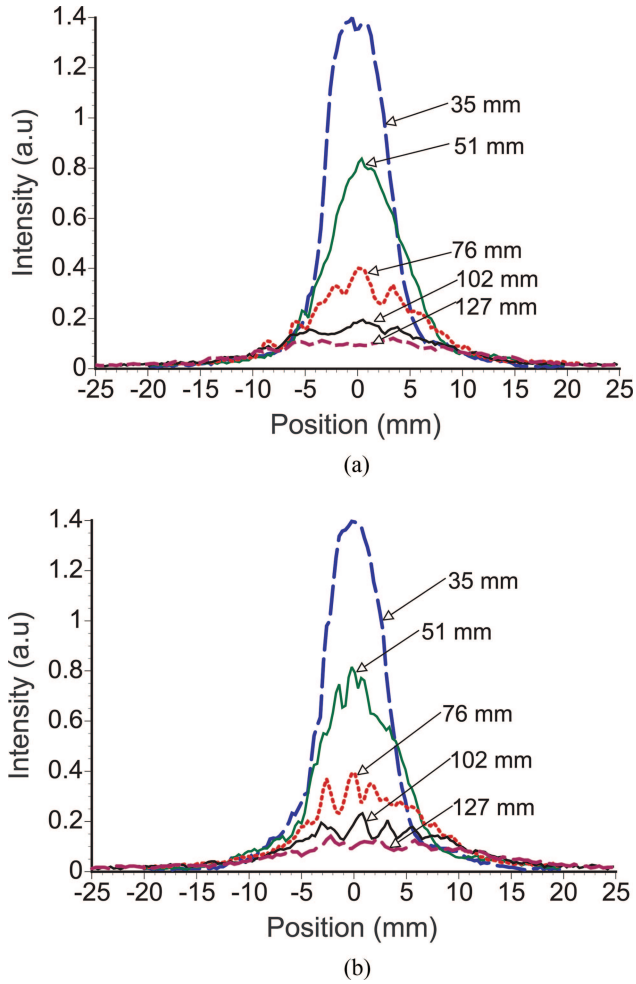

Fig. 2. (Color online) Mode profiles of the TQCL beam in (a) the horizontal and (b) the vertical directions at distances of 35, 51, 76, 102, and 127 mm from the TQCL.

bolometer entrance window was apertured to 1 mm diameter in order to obtain the necessary spatial resolution. The aperture was surrounded by anechoic material to prevent the appearance of any standing waves between the bolometer dewar and the TQCL dewar that might affect the data. The 5 mm diameter bolometer element is positioned approximately 12 mm behind the dewar window, with no internal collection optics. The horizontal and vertical profiles at varying distances from the source are shown in Figs. 2(a) and 2(b). As can be seen, the profile has a multimode structure. The beam divergence is approximately 17°.

4. Motivation and Waveguide Theory

The impetus for using hollow core dielectric waveguides to shape the TQCL beam comes from their wide application in optically pumped submillimeter-wave molecular lasers where, in contrast to metal waveguides, they provide excellent transverse mode control [21]. Single transverse mode, Gaussian profile output is readily obtained with large volume dielectric waveguides, where ratios of core tube diameter, d, to wavelength, λ, exceed 100/1. Radiation propagates inside the hollow core; hence lossy waveguide material is no impediment, and in fact is useful by reducing interference effects between reflections from the inner and outer surfaces of the tube.

Dielectric waveguide theory was developed by Stratton [22] and Snitzer [23]. They determined the field components of the low-loss modes of the most general circular cylindrical structure for the case where the radius, a, of the waveguide is much larger than the free-space wavelength, λ ($a > \lambda$), keeping terms up to order λ/a. Later these results were applied to hollow cylindrical waveguides by Marcatili and Schmeltzer [24] and Degnan [25].

Basically, there are three types of modes in such structures: transverse circular magnetic TM_{0m} modes, transverse circular electric TE_{0m} modes, and nontransverse hybrid EH_{nm} modes. The expressions for these modes [24] are greatly simplified by considering a waveguide with a large radius ($a \gg \lambda$) and ignoring terms of order λ/a. Within this approximation the EH_{1m} modes are transverse and linearly polarized, and the field distributions inside the guide are given in Ref. 25. The attenuation constant in dB/m is

$$\alpha_{nm} = 8.686\left(\frac{u_{nm}}{2\pi}\right)^2 \frac{\lambda^2}{a^3}\,\mathrm{Re}(\nu_n) \quad (\mathrm{dB/m}), \tag{1}$$

where u_{nm} is the mth root of the equation $J_{n-1}(u_{nm}) = 0$ and

$$\nu_n = \begin{cases} \dfrac{1}{\sqrt{N^2-1}} & \text{for } TE_{0m} \text{ modes } (n=0) \\ \dfrac{N^2}{\sqrt{N^2-1}} & \text{for } TM_{0m} \text{ modes } (n=0), \\ \dfrac{N^2+1}{2\sqrt{N^2-1}} & \text{for } EH_{nm} \text{ modes } (n\neq 0) \end{cases} \tag{2}$$

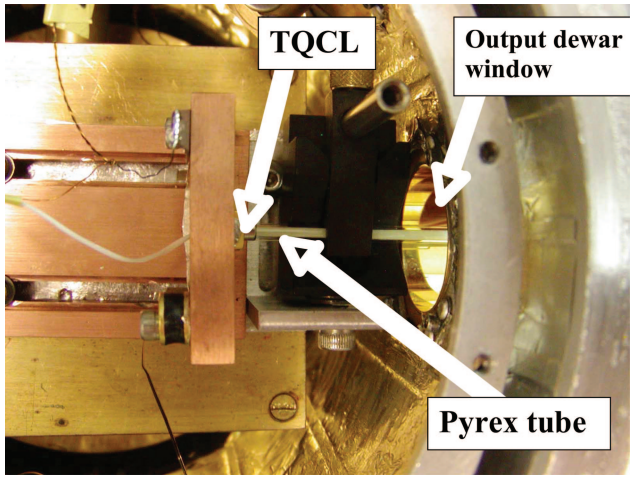

Fig. 3. (Color online) Photo of the tube mounted inside the temperature controlled LHe dewar.

where $N = \sqrt{\varepsilon_1/\varepsilon_0}$ is the complex index of refraction of the tube material [21]. The attenuation constant for a given mode varies as λ^2/a^3, so a waveguide with a larger radius has lower loss. Also, a lower order mode has lower loss than a higher order one because of the $(u_{nm})^2$ dependence.

The near- and far-field mode patterns for the low order modes radiating from the open end of a dielectric waveguide have been computed numerically by Degnan [26]. The far field pattern of the EH_{11} mode, shown in Fig. 3 in Ref. 26, is circularly symmetric, linearly polarized, and strongly resembles a Gaussian profile.

5. Experiment for Transforming the Terahertz Quantum Cascade Laser Beam Profile

The multimode TQCL beam pattern is unsuitable for applications where a high quality Gaussian beam is required. Here we demonstrate that a simple dielectric waveguide approach gives very good results in transforming the TQCL output into a Gaussian.

A Pyrex tube with an inner diameter of 1.8 mm and a length of 43 mm was used in this experiment. The laser was moved back to allow room for the waveguide, whose dimensions were chosen to produce about 1 dB of attenuation in the EH_{11} mode. The tube was mounted inside the temperature controlled dewar as close as possible to the exit facet of the TQCL without actually touching it (Fig. 3). The tube was aligned with the TQCL emission along the axis of the tube, for optimum coupling of the TQCL beam into the waveguide. The distance between the exit face of the tube and the dewar output window was 7.5 mm. The laser was driven at the same default values discussed in Section 3.

The beam profiles were obtained in exactly the same manner as before by scanning the Si LHe bolometer. The horizontal and vertical profiles were collected at varying distances from the source, and the results are displayed in Figs. 4(a) and 4(b). The po-

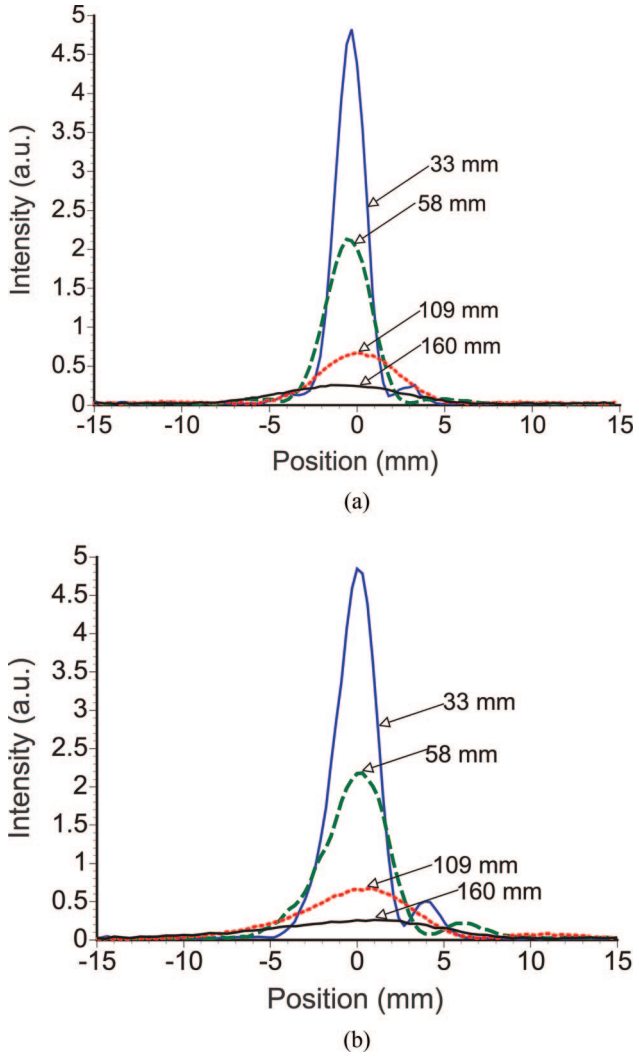

Fig. 4. (Color online) Mode profiles of the TQCL beam in (a) the horizontal and (b) the vertical directions at distances of 33, 58, 109, and 160 mm from the exit of the tube after transformation by the dielectric waveguide.

larization was also measured and determined to be unaffected by the waveguide.

To estimate the efficiency of the Pyrex waveguide, two relative values of power were measured with the bolometer. The first was obtained with the off-axis paraboloidal reflector collecting all the radiation emerging from the TQCL dewar window and focusing it into the bolometer. The TQCL was located 25 mm inside the dewar, giving a collection angle of approximately one radian. This configuration was sufficient to collect most of the power radiated by the TQCL. The second was measured when the TQCL beam had just emerged from the waveguide. The ratio gives an estimate of the waveguide efficiency with respect to power, which in this case was 35%, or −4.4 dB.

6. Predicted Mode Pattern and Experimental Results

For a Pyrex tube of 0.9 mm radius and 43 mm length, the attenuation constants of the lowest order modes at $\lambda = 101.4\ \mu m$ are, from Eq. (1),

$$\alpha_{EH_{11}} = 1.12\ \text{dB},$$

$$\alpha_{TE_{01}} = 0.97\ \text{dB},$$

$$\alpha_{TM_{01}} = 4.7\ \text{dB},$$

where for Pyrex we have used $\nu_{real} = 2.2$ and the imaginary part $\nu_{imag} = 0.05$ is neglected.

The TE_{01} mode has lower loss than the EH_{11} for a Pyrex tube, but the TQCL source is linearly polarized, and, as a result, the EH_{11} mode is preferentially excited, since the EH_{11} mode is also linearly polarized. The TM_{01} mode has much higher attenuation and it is not linearly polarized, so coupling between the TQCL source and the TM_{01} mode is very poor. Thus, we expect the EH_{11} mode to be dominant inside the tube. Abrams [27] predicts that the EH_{11} mode couples 98% of its energy to the TEM_{00} lowest order Gaussian free-space mode provided that $\omega_0/a = 0.6435$. In this case the waist ω_0 of the TEM_{00} mode has maximum overlap with the EH_{11} mode in the dielectric waveguide. The results presented here show a very close agreement to this optimum ratio. Waists of the TEM_{00} mode in the horizontal and in the vertical directions are 0.75 and 0.6 mm, respectively. The positions of the waists are 2.5 and −12 mm relative to the exit of the tube. These values were obtained with a back fitting routine, which uses measured radii of the Gaussian beam at different distances to predict the position and radius of the waist. The ratios for the 0.9 mm radius tube are

$$\omega_{0h}/a = 0.83,$$

$$\omega_{0v}/a = 0.66.$$

According to Abrams [27], the ratio predicts about 91% coupling for the horizontal beam results and 98% for the vertical measurements. The beam profiles strongly resemble the Gaussian TEM_{00} mode with some sidelobe structure at least 10 dB down from the mainlobe. Also, the beam is not cylindrically symmetrical but elongated along the vertical direction by about 30%. We expect the beam symmetry can be improved and the sidelobe intensity reduced by optimizing the dielectric waveguide parameters, such as tube length, radius, and straightness. To complete the characterization of the Gaussian beam, we estimate the collimated beam distance or the Rayleigh range (z_R) and the far-field angular beam spread θ. Using an average waist size of 0.67 mm,

$$z_R = \pi\omega_0^2/\lambda = 14\ \text{mm},$$

$$\theta = 2\lambda/\pi\omega_0 = 0.095\ \text{rad} = 5.4°.$$

As calculated in the previous section, the waveguide efficiency was −4.4 dB. Since the tube itself attenuates 1.12 dB for EH_{11} mode, the efficiency of coupling the TQCL radiation into the waveguide is −3.3 dB.

7. Conclusion

It has been demonstrated in this paper that a simple nonoptimized dielectric tube works as a very good EH_{11} filter and can transform the TQCL multimode beam into the free-space TEM_{00} mode with a relatively high efficiency. This simple approach should enable THz QC lasers to be employed in applications where a spatially coherent beam is required.

This work was supported by the U.S. Army National Ground Intelligence Center and the Department of Homeland Security. Sandia is a multiprogram laboratory operated by Sandia Corporation, a Lockhead-Martin Company, for the United States Department of Energy's National Nuclear Security Administration under contract DE-AC04-94AL85000.

References

1. S. M. Kim, F. Hatami, J. S. Harris, A. W. Kurian, J. Ford, D. King, G. Scalari, M. Giovannini, N. Hoyler, J. Faist, and G. Harris, "Biomedical terahertz imaging with a quantum cascade laser," Appl. Phys. Lett. **88,** 153903 (2006).
2. J. Darno, V. Tamosiunas, G. Fasching, J. Kröll, K. Unterrainer, M. Beck, M. Giovannini, J. Faist, C. Kremser, and P. Debbage, "Imaging with a terahertz quantum cascade laser," Opt. Express **12,** 1879–1884 (2004).
3. A. A. Kosterev, R. F. Curl, F. K. Tittel, C. Gmachl, F. Capasso, D. L. Sivco, J. N. Baillargeon, A. L. Hutchinson, and A. Y. Cho, "Effective utilization of quantum-cascade distributed-feedback lasers in absorption spectroscopy," Appl. Opt. **39,** 4425–4430 (2000).
4. J. R. Gao, J. N. Hovenier, Z. Q. Yang, J. J. A. Baselmans, A. Baryshev, M. Hajenius, T. M. Klapwijk, A. J. L. Adam, T. O. Klaassen, B. S. Williams, S. Kumar, Q. Hu, and J. L. Reno, "Terahertz heterodyne receiver based on a quantum cascade laser and a superconducting bolometer," Appl. Phys. Lett. **86,** 244104 (2005).
5. J. C. Dickinson, T. M. Goyette, A. J. Gatesman, C. S. Joseph, Z. G. Root, R. H. Giles, J. Waldman, and W. E. Nixon, "Terahertz imaging of subjects with concealed weapons," in *Terahertz for Military and Security Applications IV,* D. L. Woolard, R. J. Hwu, M. J. Rosker, and J. O. Jensen, eds., Proc. SPIE **6212,** 62120Q (2006).
6. T. M. Goyette, J. C. Dickinson, J. Waldman, W. E. Nixon, and S. Carter, "Fully polarimetric W-band ISAR imagery of scale-model tactical targets using a 1.56 THz compact range," in *Algorithms for Synthetic Aperture Radar Imagery VIII,* E. G. Zelnio, ed., Proc. SPIE **4382,** 229–240 (2001).
7. H.-W. Hübers, S. G. Pavlov, A. D. Semenov, R. Köhler, L. Mahler, A. Tredicucci, H. E. Beere, D. A. Ritchie, and E. H. Linfield, "Terahertz quantum cascade laser as a local oscillator in a heterodyne receiver," Opt. Express **13,** 5890–5896 (2005).
8. B. S. Williams, S. Kumar, Q. Hu, and J. L. Reno, "High-power terahertz quantum-cascade lasers," Electron. Lett. **42,** 89–90 (2006).
9. A. Barcan, F. K. Tittel, D. M. Mittleman, R. Dengler, P. H. Siegel, G. Scalari, L. Ajili, J. Faist, H. E. Beere, E. H. Linfield, A. G. Davies, and D. A. Ritchie, "Linewidth and tuning characteristics of terahertz quantum cascade lasers," Opt. Lett. **29,** 575–577 (2004).
10. E. Bründermann, M. Havenith, G. Scalari, M. Giovannini, J. Faist, J. Kunsch, L. Mechold, and M. Abraham, "Turn-key compact high temperature terahertz quantum cascade lasers: imaging and room temperature detection," Opt. Express **14,** 1829–1841 (2006).
11. A. J. L. Adam, I. Kašalynas, J. N. Hovenier, T. O. Klaassen, J. R. Gao, E. E. Orlova, B. S. Williams, S. Kumar, Q. Hu, and J. L. Reno, "Beam patterns of terahertz quantum cascade lasers with subwavelength cavity dimensions," Appl. Phys. Lett. **88,** 151105 (2006).
12. E. E. Orlova, J. N. Hovenier, T. O. Klaassen, I. Kašalynas, A. J. L. Adam, J. R. Gao, T. M. Klapwijk, B. S. Williams, S. Kumar, Q. Hu, and J. L. Reno, "Antenna model for wire lasers," Phys. Rev. Lett. **96,** 173904 (2006).
13. B. N. Ellison, B. J. Maddison, C. M. Mann, D. N. Matheson, M. L. Oldfield, S. Marazita, T. W. Crowe, P. Maaskant, and W. M. Kelly, "First results for a 2.5 THz Schottky diode waveguide mixer," presented at the 7th International Symposium Space THz Technology, Charlottesville, Virginia, 12–14 March 1996.
14. H. Kräutle, E. Sauter, and G. V. Schultz, "Antenna characteristics of whisker diodes used as submillimeter receivers," Infrared Phys. **17,** 477–483 (1977).
15. H. R. Fetterman, P. E. Tannenwald, B. J. Clifton, C. D. Parker, W. D. Fitzgerald, and N. R. Ericson, "Far-IR heterodyne radiometric measurements with quasioptical Schottky diode mixers," Appl. Phys. Lett. **33,** 151–154 (1978).
16. A. E. Siegman, "The antenna properties of optical heterodyne receivers," Appl. Opt. **5,** 1588–1594 (1966).
17. E. N. Grossman, "The coupling of submillimeter corner-cube antennas to Gaussian beams," Infrared Phys. **29,** 875–885 (1989).
18. S. Barbieri, J. Alton, H. E. Beere, J. Fowler, E. H. Linfield, and D. A. Ritchie, "2.9 THz quantum cascade lasers operating up to 70 K in continuous wave," Appl. Phys. Lett. **85,** 1674–1676 (2004).
19. IRlabs, Inc., Tucson, Arizona, USA.
20. Thomas Keating Ltd, Billinghurst, West Sussex, England.
21. H. P. Röser, M. Yamanaka, R. Wattenbach, and G. V. Schultz, "Investigations of optically pumped submillimeter wave laser modes," Intl. J. Infrared Millim. Waves **3,** 839–868 (1982).
22. J. A. Stratton, *Electromagnetic Theory* (McGraw-Hill, 1941), Chap. 5.
23. E. Snitzer, "Cylindrical dielectric waveguide modes," J. Opt. Soc. Am. **51,** 491 (1961).
24. E. A. J. Marcatili and R. A. Schmeltzer, "Hollow metallic and dielectric waveguides for long distance optical transmission and lasers," Bell Syst. Tech. J. **43,** 1783–1809 (1964).
25. J. J. Degnan, "The waveguide laser: a review," Appl. Phys. **11,** 1–33 (1976).
26. J. J. Degnan, "Waveguide laser mode patterns in the near and far field," Appl. Opt. **12,** 1026–1030 (1973).
27. R. L. Abrams, "Coupling losses in hollow waveguide laser resonators," IEEE J. Quantum Electron. **QE-8,** 838–843 (1972).